



ARTICLE

Parameter Study on a Composite Sound-Absorbing Structure Liner in Elevator Shafts

Ting Qu, Bo Wang and Hequn Min*

Key Laboratory of Urban and Architectural Heritage Conservation of Ministry of Education, School of Architecture, Southeast University, Nanjing, 210096, China

*Corresponding Author: Hequn Min. Email: hqmin@seu.edu.cn

Received: 19 October 2022 Accepted: 23 December 2022 Published: 20 July 2023

ABSTRACT

With the growing global environmental awareness, the development of renewable and green materials has gained increased worldwide interest to substitute conventional materials and are favorable for sustainable economic development. This paper proposed a novel eco-friendly sound absorbing structure (NSAS) liner for noise reduction in elevator shafts. The base layer integrated with the shaft walls is a damping gypsum mortarboard, and a rock wool board and a perforated cement mortarboard are used to compose the NSAS. Based on the acoustic impedance theory of porous materials and perforated panels, the sound absorption theory of the NSAS was proposed; the parameter effects of the rock wool board (flow resistivity, porosity, structure factor) and perforated panel (perforated rates, thickness, density, perforated diameter) on NSAS absorption were discussed theoretically for absorption improvement, and experiments were also conducted. Numerical results showed that the perforation rate, the thickness of the perforated plate, and the porosity, flow resistance, and volume density of the rock wool board played a key issue in the absorption performances of the NSAS. Experiments verified the accuracy of the proposed theoretical model. Wideband sound absorption performance of the NSAS at frequencies between 500–1600 Hz was achieved in both numerical analysis and experiments, and the sound absorption coefficient was improved to 0.72 around 1000 Hz after parameter adjustments. The NSAS proposed in this paper can also be made of other renewable materials with preferable structure strength and still has the potential to broaden the absorption bandwidth. It can provide a reference for controlling the elevator shaft noise.

KEYWORDS

Elevator shafts; sound-absorbing liner; porous material; flow resistivity; acoustic impedance

1 Introduction

To relieve the threat of wastes in modern urban, using renewable materials has been considered an effective strategy to reduce the quantity of accumulative plastic wastes. For instance, biodegradable materials [1], renewable biobased materials [2], renewable polymeric materials [3], biomass-derived renewable carbon material [4,5] are widely utilized to substitute conventional materials and are favorable for sustainable economic development. Multiscale architected porous materials, for example, can offer optimized energy conversion and storage opportunities due to their controllable porosity, high surface area to-volume ratio, large pore volume, and topological tunability of their underlying architecture [6].



Porous materials can also be utilized for sound absorption in noise control engineering. Due to the sound absorption mechanism, porous materials can be made of a variety of renewable materials, such as metal, as long as the porous material has internal and external connected pores. In many practical applications, a porous layer usually need to be covered by a perforated facing (i.e., a hard perforated panel) to protect the porous material and improve the surface stiffness of the structure. The so-called perforated panel is another type of sound absorbing structure, which is composed of the surface perforated panel and the backed air cavity. The perforated panel can also be made of any renewable materials with preferable structure strength, such as metal, biodegradable plastic, and renewable polymeric materials.

Elevator shaft noise is one of the main pollution sources in the residential environment. Since some of the living rooms and bedrooms are adjacent to the elevator shaft, noise and vibration occur during elevator operations and propagate into the indoor environment, negatively impacting people's life and health [7,8]. For this reason, it is important to solve the problem of effectively controlling the noise of elevator shafts in buildings. In recent years, with increasing demand for sound environment quality, numerous efficient sound absorption and vibration reduction techniques have been proposed [9–12]. Sound-absorbing materials and structures are widely used in noise control [13–15]. As a sound-absorbing material with low density and environmental protection, rock wool board material has been applied to the compound structure of building envelope, partition wall, and engineering sound absorption and noise reduction [16]. Because the rock wool has countless micro holes composed of air, particle vibration velocity varies with time and space in sound propagation. The velocity gradient causes the viscous force and internal friction between neighboring particles interacting with each other, which hinder the motion of the particles. Thus, sound energy is continuously converted into heat energy. In addition, the temperature gradient is caused by the temperature and the different densities of the particles in the sound-propagating medium. Heat transfer occurs between adjacent particles, and the sound energy is constantly transformed into heat energy. When sound-absorbing materials are combined with other materials, the sound-absorbing performance of this kind of composite sound-absorbing structure can be improved [17–19], especially at low frequencies [20–22]. In addition, in order to improve the vibration resistance of the composite sound absorption structure, a damping layer in the NSAS can effectively enhance the mechanical properties and damping characteristics of the structure [23,24].

Using Helmholtz resonators is also a basic method to increase the absorption coefficient of absorbers [25–28]. Liu et al. [29] proposed a gradually perforated porous material backed by a Helmholtz resonant cavity. The gradually perforated porous material was divided into a series of thin layers, and the acoustic properties of each layer were modeled by the double porosity theory. To achieve the surface acoustic impedance of the absorber, the backed Helmholtz resonant cavity and the connection between these thin layers were modeled by applying the transfer matrix method. Results showed that the gradually perforated hole substantially improved the impedance match between the material and air to enhance broadband sound absorption. Meanwhile, the backed Helmholtz resonant cavity brought a low-frequency sound absorption peak to augment sound absorption. The proposed absorber led to an excellent combination of low-frequency and broadband sound absorption. Li et al. [30,31] proposed a novel type of thin and lightweight sound absorber composed of melamine foam and a hollow perforated spherical structure with extended tubes to enhance low-frequency sound absorption performance. Compared with the native melamine foam, the proposed absorber could greatly improve the low-frequency sound absorption while retaining the mid-to high-frequency sound absorption, and the thickness of the proposed absorber was less than $1/28$ of the wavelength.

Compositing with perforated panels and porous materials is another method of improving the absorption performance of absorbers. Peng [32] proposed an acoustical unit composed of a rigid-porous material layer with a perforated surface and predicted the sound absorption of pure tones under normal incidence at high sound pressure levels. The sound absorptive performance of the three typical configurations of the acoustical

unit was tested under different incident sound pressure levels. Results showed that the interference effect was related to the air gap width between the perforated panel and the porous layer. The air gap width changed the linear and nonlinear acoustic impedance of the unit and, consequently, the sound absorptive properties. Li et al. [21,33] proposed a compound sound absorber consisting of perforated plates with extended tubes. And different types of absorbers with various combinations with three parallel-arranged plates with extended tubes, a porous sound-absorbing material layer, and a micro-perforated panel were proposed. The proposed combinations showed superior sound absorption performance exceeding three octaves in the targeted frequency range. Other researchers [34–36] have also studied the absorption performance of perforated plates supported by porous materials and found that the composite structure has a wider bandwidth of sound absorption performance.

Using Composite absorbers with multilayer structures with different materials can significantly improve absorption performance. Kim et al. [37] proposed a double-resonance porous sound absorption structure, which could obtain the best sound absorption performance by adjusting the design parameters and improved the sound absorption performance of the middle and low-frequency band. The design method provided a certain research basis for the design of the sound absorption performance of the middle and low-frequency porous sound absorption structure. Vašina et al. [38–42] found that the change of the parameters on the sound absorption performance is large. The study provided a certain basis for the design of composite sound absorption products and a reference for the optimization of design parameters of porous sound absorption structures. Improving the sound absorption performance of elevator shafts to reduce noise interference to the environment is an important research field. Ahsanfar et al. [43] studied the sound absorption performance of a hierarchical cellular structure of the absorption device used in elevator shafts.

As stated above, to improve the sound environment quality in the indoor environment, different methods (applications of Helmholtz resonator, changing the structure of the compound absorbers, a variety of different sound-absorbing material, the combination of parameter adjustment) have been proposed to improve the sound absorption performance of absorbers, and theoretical analysis and experiments have been carried out. However, there is still a lack of relevant application work in elevator shaft noise control. Few pieces of research have been conducted on the application of reduction of noise and vibration generated by elevator operation.

This paper proposes a novel sound absorbing structure (NSAS) liner for noise control in elevator shafts, composed of a perforated plate, a rock wool board and a damping layer. The theoretical model of NSAS sound absorption coefficient is proposed and verified by experiments. Based on the model, the effects of porous board (flow resistance, porosity, and shape factor) and perforated plate (perforation rate, thickness, aperture and density) on NSAS sound absorption coefficient under normal incidence and summarized. Additionally, two samples of NSAS were proposed based on the theoretical model.

2 Theory

2.1 Geometry of the NSAS

As shown in Fig. 1a, the NSAS consists of a perforated panel, a sound absorption board, and a damping sound insulation layer. The bottom and surface of the sound absorption board are bonded with cement mortar and damping gypsum mortar respectively, by mechanical smearing technology. The perforated surface of the NSAS has been strengthened with alkali-resistant mesh cloth or glass fiber cement. In Fig. 1b, the NSAS is located inside and outside of the concrete of the elevator shaft, and is connected by concrete slurries and embedded anchors. The NSAS forms an integrated system with the concrete. The installation process would be optimized and is superior to traditional ways by using the NSAS, improving the safety and convenience of the construction and the sound absorption performance of the elevator shaft.

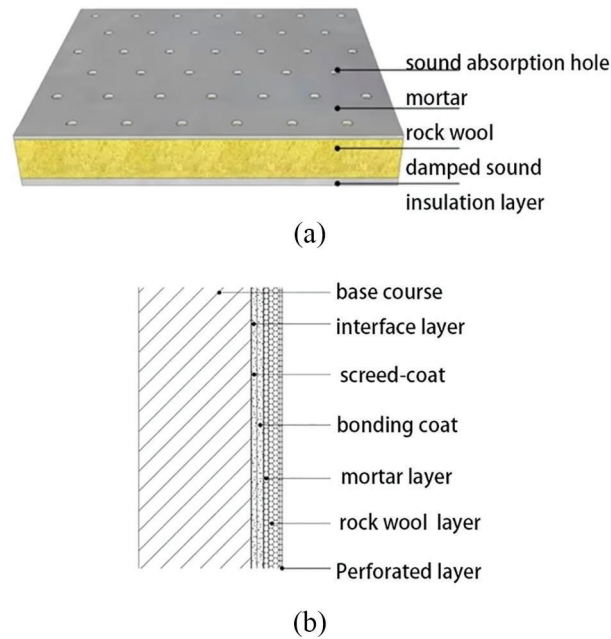


Figure 1: (a) A diagram of the novel sound absorbing structure for noise reduction; (b) the application of the novel sound absorbing structure liner in elevator shafts

2.2 Theory Model

Viscosity, internal friction, and heat conduction effects lead to the sound absorption of porous materials. When the sound waves, there is a velocity gradient in the particle vibration, and viscosity or internal friction between adjacent particles hinders particle movement and converts the sound energy into heat energy. Additionally, due to the different densities of the media particles in the process of sound wave propagation, the temperature of the media is also different, resulting in a temperature gradient and heat conduction between adjacent particles, and sound energy converts into heat energy. Parameters affecting the absorption performance of porous materials include flow resistivity, porous rates, pore shape factor, and panel thickness. According to the sound-absorbing theory proposed by Attenborough [44], the specific impedance characteristics of porous materials without a backed air cavity can be expressed as:

$$Z_N = Z_a \coth(jk_a d) \quad (1)$$

$$Z_a = \left(\frac{4T}{3\Omega} - \frac{4j\Omega\sigma_e}{2\pi f \rho_0} \right) \left(\frac{2\pi f}{ck_a} \right) \quad (2)$$

$$k_a = \frac{2\pi f}{c} \sqrt{\gamma \left(aT - \frac{4j\Omega^2\sigma_e}{2\pi f \rho_0} \right)} \quad (3)$$

In Eqs. (1)–(3), Z_N is the specific characteristic impedance of the porous material with or without backed air cavity (no airflow); Z_a and k_a represent the characteristic of specific impedance and the propagation constant inside the porous material, respectively; j is the imaginary unit; Parameter a is defined by $a = 4/3 - [(\gamma - 1)/\gamma]N_{pr}$, where N_{pr} is the Prandtl number and can be 0.71 at room temperature; c , d , Ω , and T are the speed of sound in air, thickness of the porous panel, porosity, and tortuosity inside the media, respectively; f is the frequency in Hz; ρ_0 and γ denote the density and the ratio of specific heats of air, separately; σ_e denotes the effective flow resistivity, and is defined as follows [45]:

$$\sigma_e = 4S_p S_p \sigma / \Omega \quad (4)$$

In Eq. (4), S_p is the pore shape factor; σ is the flow resistivity of the media with a unit of cgs ($1 \text{ cgs} = 1 \text{ kPa}\cdot\text{sm}^{-2}$).

When a perforated plate covers the surface of porous material, extra absorption is achieved at low frequencies due to the absorption mechanism of perforated panels and the backed air cavity, and the so-called NSAS is formed. Perforated plates and the air cavity behind the plates can form a resonance sound absorption structure, which can be regarded as multiple paralleled-arranged Helmholtz resonators. When the frequency of the incident sound is consistent with the resonance frequency of the structure, intense vibration and friction will be generated at perforated necks to strengthen the sound absorption and form the sound absorption peak. Parameters affecting the perforated plate's absorption performance include plate thickness, aperture, perforation rates, and plate density. When the backed air cavity is filled with porous materials, the resonance peak moves to higher frequencies, improving the sound absorption coefficient. When a perforated plate covers the porous liner, the characteristic impedance of the NSAS surface can be expressed as [46]:

$$Z_{NP} = Z_N + \frac{\frac{100}{P} \{j\rho c \tan[kl_e(1-M)] + R_a A\}}{1 + \frac{100}{j\omega m P} \{j\rho c \tan[kl_e(1-M)] + R_a A\}} \quad (5)$$

where

$$R_a = \frac{l}{\pi a^3} \sqrt{2\eta\omega\rho_0} \quad (6)$$

It should be noted that the Eq. (5) is established on the basis of electro-acoustic analogies. It is a useful method for the solution of many tasks in acoustics by describing the relationship between acoustic elements with electrical circuit and thus obtaining the characteristics of the acoustic system.

And the normal incidence sound absorption coefficient of the NSAS can be defined as:

$$\alpha = \frac{4\text{Re}(Z_{NP})}{(\text{Re}(Z_{NP}) + 1)^2 + \text{Im}(Z_{NP})^2} \quad (7)$$

In Eq. (5), Z_{NP} is the surface characteristic impedance of NSAS, and l_e , ω , P , R_a represent the effective length of each perforated hole, angular frequency, perforated rates, acoustic resistance of each perforated hole, respectively; Parameters A , M and m are the sizes of each perforated hole, the Mach number of airflow through perforated holes, and mass per unit area of the perforated plate, respectively. In Eq. (6), a , l , and η denote perforated diameter, length of a perforated hole, and shear viscosity coefficient of air; $k = 2\pi f/c$ is the wave number.

3 Numerical Discussions

3.1 Effects of NSAS Parameters on Sound Absorption Performance

Numerous parameters affect the sound absorption performance of the NSAS, including flow resistivity, porosity, and pore shape factor of the porous material as well as perforation rates, perforated diameter, panel thickness, and density of the perforated panel. This section discusses the effects of the above parameters on the sound absorption performance of the NSAS based on the analytical theory proposed in Section 2. The parameter range of the NSAS used in the numerical discussions is shown in Table 1.

Table 1: Parameter settings in the numerical discussions on the effects of parameters on absorption coefficients of the composite structure

Parameters of porous material				Parameters of perforated panel			
Flow resistivity/ cgs	Porous rates	Pore shape factor	Thickness	Perforated rates/%	Thickness	Diameter of perforated holes/mm	Density/ kg/m ³
50–600	0.9	2	13	4	6	8	450
400	0.001–0.9	2	13	4	6	8	450
400	0.9	1–9	13	4	6	8	450
400	0.9	2	10–50	4	6	8	450
400	0.9	2	13	4–34	6	8	450
400	0.9	2	13	4	1–9	8	450
400	0.9	2	13	4	6	0.6–8	450
400	0.9	2	13	6	6	8	450–1050

The effects of parameters of porous material on the sound absorption coefficient of the NSAS are studied, and the overall thickness of the NSAS is set as 28 mm. As for the flow resistivity (from 50 to 600 cgs) shown in Fig. 2a, the absorption coefficient increases significantly with the increase of flow resistivity, and the absorption peak is located at 540 Hz. For the porosity (from 0.001 to 0.9), as shown in Fig. 2b, with the increase of porosity, the absorption coefficient decreases, and the absorption peak moves to lower frequencies. For the pore shape factor (from 1 to 9), as shown in Fig. 2c, with the increase of shape factor, the sound absorption coefficient increases significantly, and the absorption peak moves to higher frequencies. As for the thickness of the sound absorbing material (10–50 mm), the composite structure's sound absorption coefficient increases with the thickness of porous material layer. The effects are particularly significant at low frequencies, while limited at high frequencies. However, limited effects can also be observed by theoretical analysis, when large thickness of the composite, such as more than 200 mm, is adopted.

The effect of perforated panel parameters on the sound absorption performance of the NSAS is conducted, and the overall thickness of the NSAS is set as 28 mm. For the perforated rate (from 4% to 34%), as shown in Fig. 3a, the absorption coefficient increases significantly with the increase of perforation rate, and the absorption peak shifts to higher frequencies. For the panel thickness (from 1 to 9 mm), as shown in Fig. 3b, with the increase of thickness, the absorption coefficient decreases and the absorption peak moves to lower frequencies. As for the perforation diameter (from 0.6 to 8 mm), as shown in Fig. 3c, the absorption coefficient increases slightly, and the absorption peak moves to higher frequencies. For the perforated panel density (from 450 to 1050 kg/m³), as shown in Fig. 3d, with the increase of density, the sound absorption coefficient decreases slightly, and the absorption peak shifts slightly to lower frequencies.

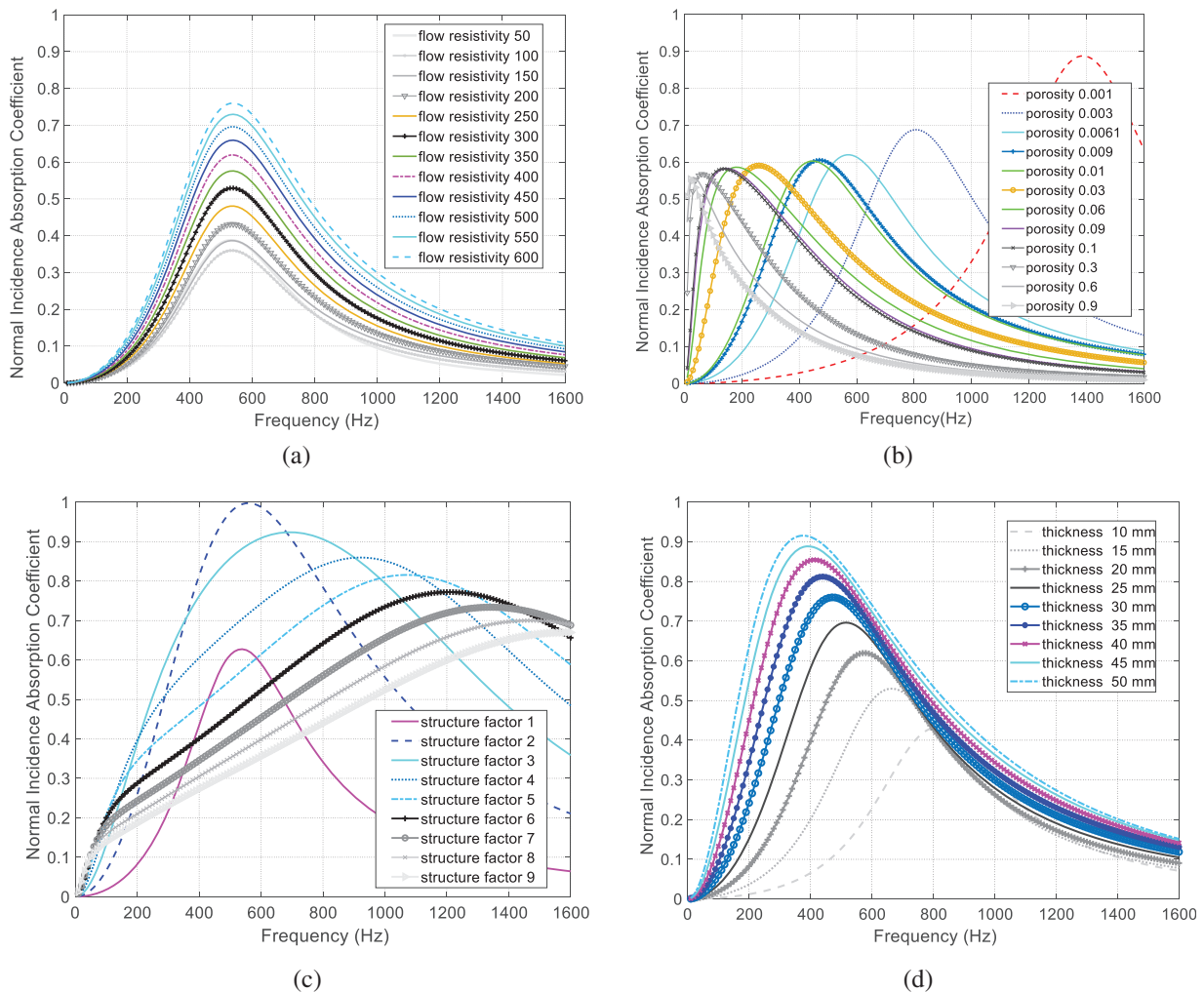


Figure 2: Sound absorption coefficients of the NSAS with different porous parameters of (a) flow resistivity, (b) porosity, (c) shapefactor, (d) thickness

3.2 Summaries on Parameter Effects

The effects of parameters on sound absorption performance of the NSAS are summarized in [Table 2](#) based on the analytical results in [Section 3.1](#). It can be seen that the parameters of porous material, as well as the perforated rate and thickness of the perforated panel, has a significant effect on absorption performance of NSAS, while the density of the perforated panel shows slight effects. The preferable absorption coefficient can be thus obtained by determining the suitable values of each parameter of the NSAS. In addition, noise peak frequency in the elevator shaft can be determined by measurements, which is the corresponding frequency where the absorption peak of the composite structure is located. Finally, the absorption peak of the composite structure can be accurately designed and optimized based on the analytical model in [Section 2.2](#), and the findings in [Section 3.1](#) conclude this work.

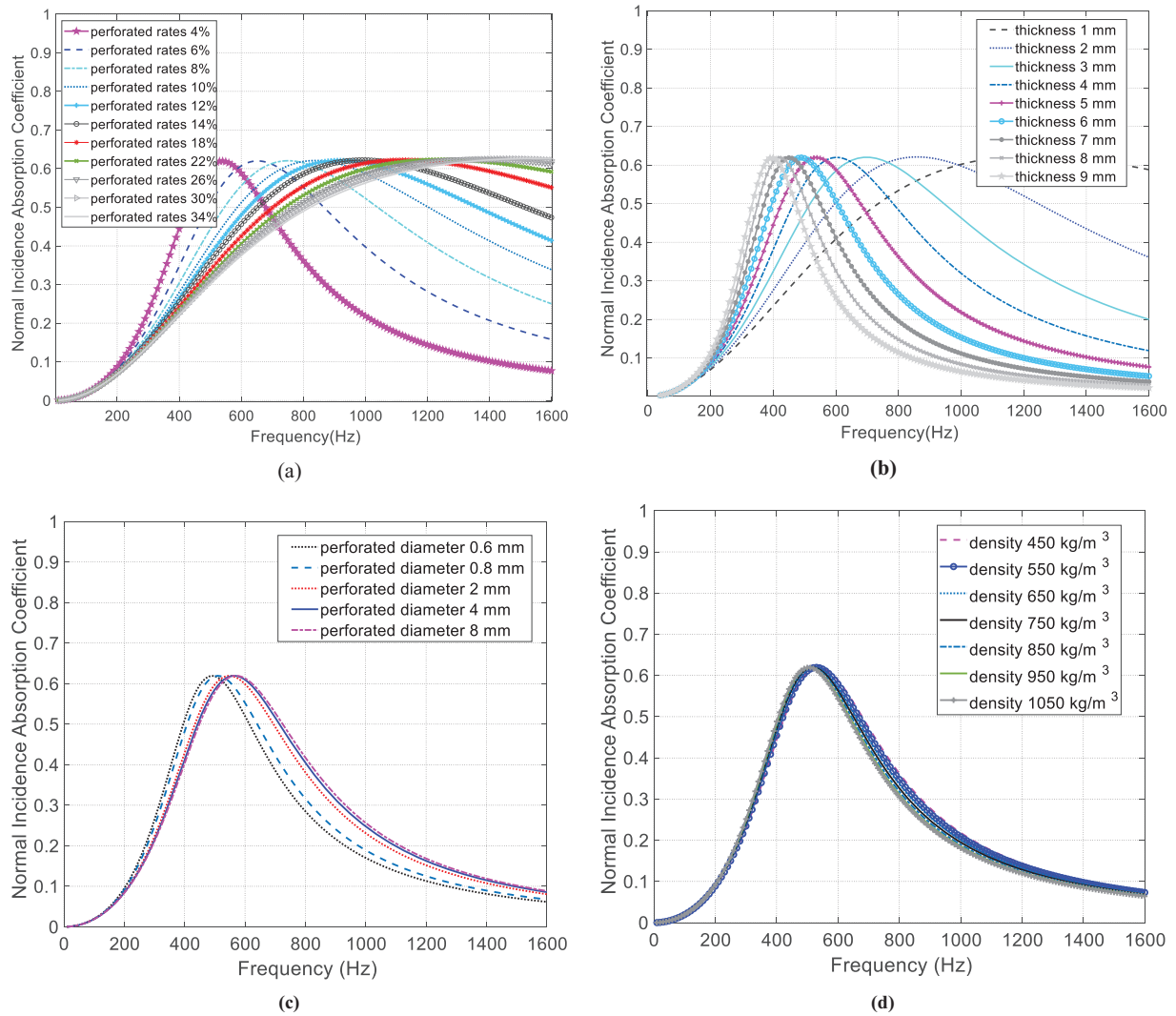


Figure 3: Sound absorption coefficients of the NSAS with different perforated panel parameters of (a) perforated rate, (b) thickness, (c) perforated diameter, and (d) density

Table 2: Summaries of the effects of the NSAS parameters on sound absorption coefficient

	Parameters	The influence on sound absorption coefficient
Porous material layer	Flow resistivity	Appropriate values of flow resistivity are suggested to be used for good absorption performance
	Porosity	Absorption performance gets weaker when dense materials with low porosity are utilized
	Pore shape factor	When the value of flow resistivity is very small, periodic changes of the absorption coefficient can be seen at mid-high frequencies with the increase of the pore shape factor Slight impact at low frequencies

(Continued)

Table 2 (continued)		
	Parameters	The influence on sound absorption coefficient
	Rock wool boardthickness	The sound absorption coefficient of the composite structure increases with the increase of the thickness of porous material layer, especially at low frequencies, while the effect at high frequencies is limited. However, limited effects can also be observed by theoretical analysis when large thickness of the composite, such as more than 200 mm, is adopted.
Perforated panel	Panel thickness	Absorption performance improves at low frequencies and slight impact at high frequencies with the increase of panel thickness.
	Perforated rates	Absorption coefficient improves and absorption peak moves towards higher frequencies with the increase of the perforated rate.
	Perforated diameter	Absorption performance improves when a smaller perforated diameter is applied.
	Density	Absorption coefficient decreases slightly and absorption peak moves towards lower frequencies with the increase in density.

4 Experiments

Experiments are conducted to measure the normal incident absorption coefficient of the NSAS on the basis of the two-microphone transfer function method according to the standard ISO 10534-2 [47]. The impedance tube with a rectangular cross section is shown in Fig. 4a. Hard acrylic with a cross section size of 100 mm × 100 mm and a thickness of 15 mm constitutes the experimental frame. The front tube of the standing wave tube is connected with the sound source, and one end of the back tube is the closed end of the specimen. The first cut-on frequency in this duct is about 1700 Hz, with the effective measurement range from 50 to 1600 Hz. A photo of the experimental equipment is shown in Fig. 4b. Two 1/2-inch G.R.A.S Type 40AP microphones are mounted on the duct wall flush with the interior surface of the wall to measure the acoustic pressures inside the duct. The distance between the two microphones is 5 mm. A 3.5-inch HiVi-M3S Type loudspeaker is installed at the end of the duct and driven by a B&K 2716 Type amplifier. The sample under test is mounted on the other end of the duct. The sound signal is generated and processed by the B&K PULSE 3560D system. The NSAS sample should not be excessively compressed, nor should it be installed too tightly so that the sample is extruded and deformed. The gaps around the sample are blocked by plasticine to make the sample installation more stable. Parameters of the two NSAS cases used in experiments are given in Table 3.

Sound absorption coefficients of two NSAS cases are presented in Fig. 5 by theoretical prediction and experiment. The corresponding parameters are given in Table 3. It can be seen that the measured results showed good agreement with the predicted results, indicating the reliability of the analytical model of the NSAS in predicting the sound absorption coefficient. A sharp absorption peak with a frequency of 500 Hz and an absorption coefficient of 0.6 can be seen in case 1, with the effective absorption range (absorption coefficient larger than 0.5) between 400–650 Hz. The improved absorption performance showed that the value of the absorption peak reached 0.7 with a wide absorption bandwidth and the effective frequency range of 400–1600 Hz, indicating the efficiency of absorption performance improvement of case 2 according to the parameter effects in Table 3. Results also showed that reducing

the thickness of the perforated panel or increasing the thickness of the basic layer could broaden absorption bandwidth and enhance absorption coefficient. In addition, case 2 has a set of parameters that are more conducive to improving the sound absorption coefficient of NSAS based on the above parameter discussion. Through the simulation and experimental comparison between case 2 and case 1, it can be found that the sound absorption parameters of case 2 effectively improve the sound absorption performance of NSAS, and it is a relatively optimal parameter combination.

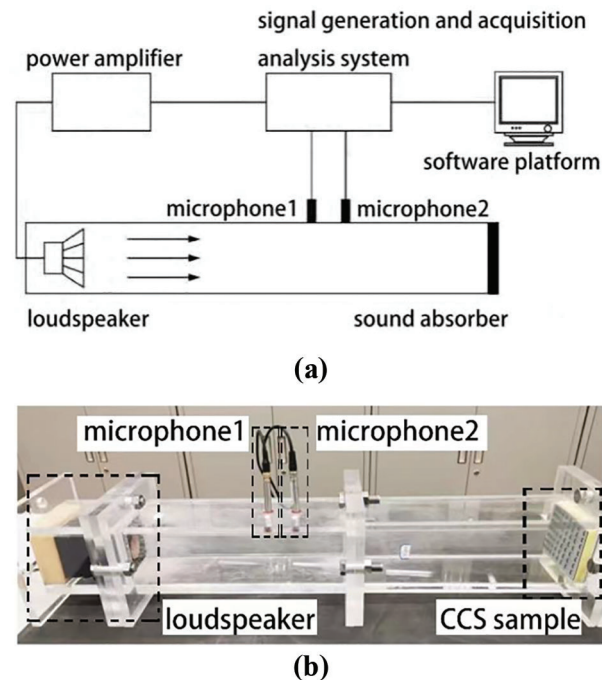


Figure 4: (a) A schematic diagram of the experiment in impedance tube; (b) a photograph of the experiment

Table 3: Parameters of the NSAS cases

	Parameters of perforated panel				Parameters of porous material			
	Thickness of perforated panel/mm	Perforated rates/%	Diameter of perforated holes/mm	Density/ kg/m^3	Flow resistivity/cgs	Pore shape factor	Porous rates	Thickness/mm
Case 1	6	4	8	450	400	2	0.9	13
Case 2	2	25	8	450	550	3.011	0.7	17

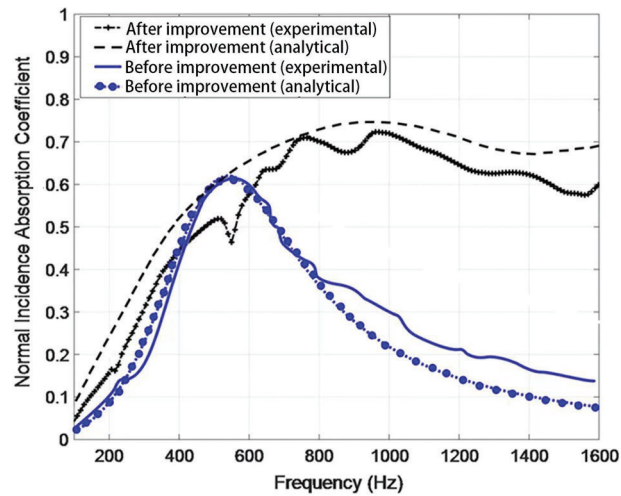


Figure 5: Measured normal incidence sound absorption coefficients of the two NSAS cases

5 Conclusions

This study proposed a composite sound-absorbing structure composed of a perforated panel and porous material layer, which could be applied to the inner wall of the elevator shaft for noise reduction. Due to the sound absorption mechanism, this kind of sound absorbing structure can be made up of any renewable materials with preferable structure strength, which not only facilitates sustainable economic development but also provides sustainable life for our next generation. Specifically, the sound absorption structure in this paper is composed of a rock wool board as porous material layer and a cement mortar perforated board. The analytical model on the composite structure's normal incidence sound absorption coefficient was proposed and validated. This study generated the following conclusions are summarized as follows:

As for the perforated plate, the perforation rate had the greatest impact on the sound absorption performance, followed by thickness, aperture and density of the plate.

As for the porous material, the flow resistance had the greatest impact on the sound absorption performance, followed by the porosity and structure factor.

By increasing the thickness, decreasing the perforation rates of the perforated plate, or increasing the porosity of the porous material, the absorption performance of the NSAS at low frequencies could be improved.

The normal incident sound absorption coefficients of the improved NSAS can reach 0.72 around 1000 Hz. By changing the parameters, the sound absorption bandwidth could be widened.

For actual engineering applications, noise peak frequency in the elevator shaft can be determined by measurements, which is the corresponding frequency where the absorption peak of the composite structure is located. Finally, the absorption peak of the composite structure can be accurately designed and improved on the basis of the numerical finding in this paper.

Funding Statement: This work is supported by Opening Foundation of Key Laboratory of New Technology for Construction of Cities in Mountain Area, Ministry of Education, China (LNTCCMA-20210104). This work was also supported by the Natural Science Foundation of China (Grant No. 51408113) and the Natural Science Foundation of Jiangsu Province, China (Grant No. BK20140632).

Conflicts of Interest: The authors declare that they have no conflicts of interest to report regarding the present study.

References

1. Huang, K., Chueh, C., Chen, W. (2021). Recent advance in renewable materials and green processes for optoelectronic applications. *Materials Today Sustainability*, 11–12, 100057. <https://doi.org/10.1016/j.mtsust.2020.100057>
2. Zeidler, H., Klemm, D., Bottger-Hiller, F., Fritsch, S., Le Guen, M. J. et al. (2018). 3D printing of biodegradable parts using renewable biobased materials. *Procedia Manufacturing*, 21, 117–124. <https://doi.org/10.1016/j.promfg.2018.02.101>
3. Ojogbo, E., Ogunsona, E. O., Mekonnen, T. H. (2020). Chemical and physical modifications of starch for renewable polymeric materials. *Materials Today Sustainability*, 7–8, 100028. <https://doi.org/10.1016/j.mtsust.2019.100028>
4. Korbelyiova, L., Malefors, C., Lalander, C., Wikström, F., Eriksson, M. (2021). Paper vs leaf: Carbon footprint of single-use plates made from renewable materials. *Sustainable Production and Consumption*, 25, 77–90. <https://doi.org/10.1016/j.spc.2020.08.004>
5. Deng, B., Huang, Q., Zhang, W., Liu, J., Meng, Q. et al. (2021). Design high performance biomass-derived renewable carbon material for electric energy storage system. *Journal of Cleaner Production*, 309(20), 127391. <https://doi.org/10.1016/j.jclepro.2021.127391>
6. Hoseini, S. S., Seyedkanani, A., Najafi, G., Sasmito, A. P. (2023). Multiscale architected porous materials for renewable energy conversion and storage. *Energy Storage Materials*, 59(1), 102768. <https://doi.org/10.1016/j.ensm.2023.102768>
7. Daiber, A., Kröller-Schön, S., Frenis, K., Oelze, M., Kalinovic, S. et al. (2019). Environmental noise induces the release of stress hormones and inflammatory signaling molecules leading to oxidative stress and vascular dysfunction—Signatures of the internal exposome. *Biofactors*, 45(4), 495–506. <https://doi.org/10.1002/biof.1506>
8. Thompson, R., Smith, R. B., Bou Karim, Y., Shen, C., Drummond, K. et al. (2022). Noise pollution and human cognition: An updated systematic review and meta-analysis of recent evidence. *Environment International*, 158(24), 106905. <https://doi.org/10.1016/j.envint.2021.106905>
9. Gai, X. L., Xing, T., Li, X. H., Zhang, B., Cai, Z. N. et al. (2018). Sound absorption properties of microperforated panel with membrane cell and mass blocks composite structure. *Applied Acoustics*, 137(2), 98–107. <https://doi.org/10.1016/j.apacoust.2018.03.013>
10. Xie, S. C., Li, Z., Yan, H. Y., Yang, S. C. (2022). Ultra-broadband sound absorption performance of a multi-cavity composite structure filled with polyurethane. *Applied Acoustics*, 189(5), 612–625. <https://doi.org/10.1016/j.apacoust.2021.108612>
11. Ju, Z. H., He, Q., Zhan, T. Y., Zhang, H. Y., Sun, L. et al. (2019). Steam exploded peanut shell fiber as the filler in the rigid polyurethane foams. *Journal of Renewable Materials*, 7(11), 1077–1091. <https://doi.org/10.32604/jrm.2019.07525>
12. Manik, T. N., Nuki, S. A., Fauziyah, N. A., Zainuri, M. (2021). Structure, dynamic-mechanical and acoustic properties of oil palm trunk modified by melamine formaldehyde. *Journal of Renewable Materials*, 9(9), 1647–1660. <https://doi.org/10.32604/jrm.2021.016089>
13. Liu, Q. H., Liu, X. W., Zhang, C. Z., Xin, F. X. (2021). A novel multiscale porous composite structure for sound absorption enhancement. *Composite Structures*, 276(7), 114456. <https://doi.org/10.1016/j.compstruct.2021.114456>
14. Ryoo, H., Jeon, W. (2022). Broadband sound absorption using multiple hybrid resonances of acoustic metasurfaces. *International Journal of Mechanical Sciences*, 229, 107508. <https://doi.org/10.1016/j.ijmecsci.2022.107508>
15. Meriç, C., Erol, H., Özkan, A. (2016). On the sound absorption performance of a felt sound absorber. *Applied Acoustics*, 114(3), 275–280. <https://doi.org/10.1016/j.apacoust.2016.08.003>
16. Mohammadi, B., Ershad-Langroudi, A., Moradi, G., Safaiyan, A., Habibi, P. (2022). Mechanical and sound absorption properties of open-cell polyurethane foams modified with rock wool fiber. *Journal of Building Engineering*, 48(11), 103872. <https://doi.org/10.1016/j.jobbe.2021.103872>

17. Ren, S. W., Liu, Y. Y., Sun, W., Wang, H., Lei, Y. et al. (2022). Broadband low-frequency sound absorbing metastructures composed of impedance matching coiled-up cavity and porous materials. *Applied Acoustics*, 200(15), 109061. <https://doi.org/10.1016/j.apacoust.2022.109061>
18. Lagarrigue, C., Groby, J. P., Tournat, V., Dazel, O., Umnova, O. (2014). Absorption of sound by porous layers with embedded periodic arrays of resonant inclusions. *The Journal of the Acoustical Society of America*, 134(6), 4670–4680. <https://doi.org/10.1121/1.4824843>
19. Li, X., Liu, B. L., Chang, D. Q. (2021). An acoustic impedance structure consisting of perforated panel resonator and porous material for low-to-mid frequency sound absorption. *Applied Acoustics*, 180(1), 108069. <https://doi.org/10.1016/j.apacoust.2021.108069>
20. Kim, B. S., Park, J. (2018). Double resonant porous structure backed by air cavity for low frequency sound absorption improvement. *Composite Structure*, 183, 545–549. <https://doi.org/10.1016/j.compstruct.2017.06.027>
21. Li, D. K., Chang, D. Q., Liu, B. L. (2017). Enhanced low- to mid-frequency sound absorption using parallel-arranged perforated plates with extended tubes and porous material. *Applied Acoustics*, 127(2), 316–323. <https://doi.org/10.1016/j.apacoust.2017.06.019>
22. Wang, C. N., Torng, J. H. (2001). Experimental study of the absorption characteristics of some porous fibrous materials. *Applied Acoustics*, 62(4), 447–459. [https://doi.org/10.1016/S0003-682X\(00\)00043-8](https://doi.org/10.1016/S0003-682X(00)00043-8)
23. Tang, Z., Li, G. Q., Lu, S., Wang, J. P., Chi, L. (2022). Enhance mechanical damping behavior of RHA-cement mortar with bionic inorganic-organic laminated structures. *Construction and Building Materials*, 323(1), 126521. <https://doi.org/10.1016/j.conbuildmat.2022.126521>
24. Wang, X. G., Wu, L., Lu, F. (2018). Damping characteristics and interface properties of gradient structural concrete based on damping enhancement. *Journal of Building Materials*, 21(5), 780–785.
25. Culik, M., Danihelova, A., Ondrejka, V., Alac, P. (2020). Sound absorption of board construction material used in wooden buildings. *Akustika*, 37, 52–58. <https://doi.org/10.36336/akustika20203751>
26. Zhou, Y. H., Chen, S., Fu, H. Y., Mohrmann, S., Wang, Z. (2022). Sound absorption performance of light-frame timber construction wall based on Helmholtz resonator. *BioResource*, 17(2), 2652–2666. <https://doi.org/10.15376/biores.17.2.2652-2666>
27. Groby, J. P., Lagarrigue, C., Brouard, B., Dazel, O., Tournat, V. et al. (2015). Enhancing the absorption properties of acoustic porous plates by periodically embedding Helmholtz resonators. *The Journal of the Acoustical Society of America*, 137(1), 273–280. <https://doi.org/10.1121/1.4904534>
28. Chen, S., Zhou, Y. H., Mohrmann, S., Fu, H. Y., Zou, Y. Y. et al. (2022). Acoustics performance research and analysis of light timber construction wall elements based on helmholtz metasurface. *Journal of Renewable Materials*, 10(11), 2791–2803. <https://doi.org/10.32604/jrm.2022.021531>
29. Liu, X. W., Yu, C. L., Xin, F. X. (2021). Gradually perforated porous materials backed with Helmholtz resonant cavity for broadband low-frequency sound absorption. *Composite Structure*, 263(1), 113647. <https://doi.org/10.1016/j.compstruct.2021.113647>
30. Li, D. K., Jiang, Z. C., Li, L., Liu, X. B., Wang, X. F. et al. (2020). Investigation of acoustic properties on wideband sound-absorber composed of hollow perforated spherical structure with extended tubes and porous materials. *Applied Sciences*, 10(24), 8978. <https://doi.org/10.3390/app10248978>
31. Wu, L., Liu, M., Liu, X. W., Xiong, X. Z., Pang, J. X. et al. (2021). Optimal design of structural parameters of multi-layer porous sound-absorbing materials. *Journal of Applied Acoustics*, 40(3), 449–456.
32. Peng, F. (2018). Sound absorption of a porous material with a perforated facing at high sound pressure levels. *Journal of Sound & Vibration*, 425(2), 1–20. <https://doi.org/10.1016/j.jsv.2018.03.028>
33. Li, D. K., Chang, D. Q., Liu, B. L. (2016). Enhancing the low frequency sound absorption of a perforated panel by parallel-arranged extended tubes. *Applied Acoustics*, 102, 126–132. <https://doi.org/10.1016/j.apacoust.2015.10.001>
34. Babu, M. C. L., Padmanabhan, C. (2010). Noise control of a rectangular cavity using macro perforated porous-elastic materials. *Applied Acoustics*, 71(5), 418–430. <https://doi.org/10.1016/j.apacoust.2009.11.012>
35. Davern, W. A. (1977). Perforated facings backed with porous materials as sound absorbersan experimental study. *Applied Acoustics*, 10(2), 85–112. [https://doi.org/10.1016/0003-682X\(77\)90019-6](https://doi.org/10.1016/0003-682X(77)90019-6)

36. Li, D. K., Chang, D. Q., Liu, B. L., Tian, J. (2015). A perforated panel sound absorber for low frequencies. *Proceedings of 22nd International Congress on Sound and Vibration*, pp. 12–16. Florence, Italy.
37. Kim, B. S., Park, J. (2018). Double resonant porous structure backed by air cavity for low frequency sound absorption improvement. *Composite Structures*, 183, 545–549. <https://doi.org/10.1016/j.compstruct.2017.06.027>
38. Vašina, M., Hružík, L., Bureček, A., Mahdal, M., Monková, K. et al. (2019). A study of factors influencing sound absorption properties of porous materials. *Manufacturing Technology*, 19(1), 156–160. <https://doi.org/10.21062/ujep/261.2019/a/1213-2489/MT/19/1/156>
39. Liu, J., Liu, X., Bao, W., Wang, S. S., Chen, L. M. et al. (2014). The acoustic behaviors of dual layered nonwoven absorbers: From model building to experiment verification. *Journal of Computational Acoustics*, 22(2), 1450001. <https://doi.org/10.1142/S0218396X14500015>
40. Zhang, X. L., Liu, C. P. (2013). Study of a sound absorbing polyurethane based on porous composite material. *Applied Mechanics and Materials*, 1623, 275–277. <https://doi.org/10.4028/www.scientific.net/AMM.275-277.1623>
41. Yang, X., Wang, Y. S., Yu, H. W. (2006). Sound absorption properties of multilayered polymer composite for oblique incidence. *Acta Materiae Compositae Sinica*, 23(6), 21–28. [https://doi.org/10.1016/S1872-2040\(06\)60046-7](https://doi.org/10.1016/S1872-2040(06)60046-7)
42. Wang, Y. P., Wang, Y. H., Liu, Z. M., Yu, H. D., Xu, J. K. (2021). Effect of plastocene embedment in the microperforated plate on its acoustic performance. *Journal of Renewable Materials*, 9(5), 923–941. <https://doi.org/10.32604/jrm.2021.014138>
43. Ahsanfar, M., Galehdari, S. A. (2017). Optimum design for graded honeycomb as energy absorber device in elevator cabin. *Procedia Engineering*, 173, 1291–1298. <https://doi.org/10.1016/j.proeng.2016.12.163>
44. Attenborough, K. (1992). Ground parameter information for propagation modeling. *The Journal of the Acoustical Society of America*, 92(1), 418–427. <https://doi.org/10.1121/1.404251>
45. Min, H. Q., Chen, W. S., Qiu, X. J. (2011). Single frequency sound propagation in flat waveguides with locally reactive impedance boundaries. *The Journal of the Acoustical Society of America*, 130(2), 772–782. <https://doi.org/10.1121/1.3608124>
46. Bies, D. A., Hansen, C. H. (2013). *Engineering noise control theory and practice*, pp. 636–637. London and New York: Spon press Taylor Frands Group.
47. International Organization for Standardization (1998). *ISO-10534-2. Acoustics-Determination of sound absorption coefficient and impedance in impedance tubes-Part 2: Transfer-function method*. Switzerland.